Effect of negative differential conductance in graphene Esaki diodes: GNR or GNM?

V. Hung Nguyen, F. Mazzamuto, J. Saint-Martin, A. Bournel, **P. Dollfus**

Institute of Fundamental Electroniucs, CNRS, Univ. Paris-Sud, UMR 8622, Orsay, France
philippe.dollfus@u-psud.fr

The effect of negative differential conductance (NDC) has been exploited for high frequency applications in many conventional semiconductor devices [1]. These last years, this effect has been also investigated in several graphene structures [2-8]. However, due to the lack of bandgap in 2D graphene systems [2-5] or to the influence of edge defects in narrow graphene nanoribbons (GNR) [7-8], it was shown that the NDC effect is generally weak in these structures. Recently, we have demonstrated that a strong NDC effect can be achieved in graphene PN junctions [9], and especially in GNR hetero-structures with a peak-to-valley current ratio (PVR) higher than one thousand at room temperature [10].

To obtain such a strong effect, a large energy bandgap is an essential ingredient, which can be achieved, e.g., by cutting graphene into armchair GNRs or by patterning graphene nanomeshes (GNMs) where the size of nanoholes and the distance between them can be controlled down to the sub 10-nm scale [11]. Indeed, an increase of bandgap reduces strongly the valley current and may result in an increase of the PVR of NDC as proved in ref. [9]. However, such a large bandgap also results in the appearance of evanescent states in the transition region between p-doped and n-doped zones, which reduces the peak current and makes it very sensitive to the transition length.

By taking advantage of the possibilities of bandgap engineering in armchair GNRs or GNMs, we demonstrate that the NDC effect can be improved significantly in GNR PN heterojunctions wherein the bandgap is large in the two junction sides while it is small in the transition region. This configuration may be obtained in GNRs as the T-shape GNR schematized in Fig. 1. Actually, in such heterostructures the interband tunneling in the peak current regime is enhanced while the valley current is maintained small thanks to the large bandgap in the doped regions. It is illustrated in the DOS and the transmission coefficient plotted in Fig.2 for a uniform-width armchair GNR and a T-shape GNR of width characterized by the numbers of dimmers $M_C = 21$ ($E_G = 0.37$ eV) in the doped regions and $M_D = 29$ ($E_G = 0.062$ eV) in the transition region. In particular, Fig.2 shows that while the evanescent states around the neutral point in the transition region are observed clearly in the simple junction (left), they are not visible in the T-junction (right). It leads to the enhancement of the interband tunnelling in the latter case, as shown in the plot of transmission probability. The resulting I-V characteristics is displayed for three junctions in Fig. 3. While the valley current is always small, the peak current and hence the PVR increase significantly when reducing E_G. For instance, the PVR is about 1100 and 2300 for $M_D = 33$ ($E_G = 0.233$ eV) and $M_D = 29$ ($E_G = 0.062$ eV), respectively. Additionally, it is weakly sensitive to the transition length and to the edge disorder (not shown).

However, though efficient, these GNR configurations still raise a technological challenge for their manufacturing and the current is small in single GNR. Alternatively, GNM structures (Fig. 4) may provide similar effects on large sheets with high current [12]. In GNM/pristine graphene/GNM hetero-structures wherein the bandgap (of pristine graphene) in the transition region is zero, a PVR as high as few hundreds can be osberved, with a weak dependence on the transition length (Fig. 5). In this structure, the size of nanoholes and the distance between them are 3 nm and 5 nm respectively, which is not far from those already achieved experimentally [11].

These NDC effects will be discussed and compared in both cases of GNR and GNM nanostructuring.

References

[1] H. Mizuta and T. Tanoue, The Physics and Applications of Resonant Tunneling Diodes, Cambridge University Press, Cambridge (1995).

[2] V. Nam Do, V. Hung Nguyen, P. Dollfus, and A. Bournel, J. Appl. Phys. **104** (2008) 063708.

[3] H. Chau Nguyen and V. Lien Nguyen, J. Phys.: Condens. Matter **21** (2009) 045305.

[4] V. Hung Nguyen, A. Bournel, V. Lien Nguyen, and P. Dollfus, Appl. Phys. Lett. **95** (2009) 232115.

[5] G. Fiori, IEEE Electron Device Lett. **32** (2011) 1334.

[6] Z. F. Wang et al., Appl. Phys. Lett. **92** (2008) 133114.

[7] G. Liang, S. B. Khalid and K.-T. Lam, J. Phys. D: Appl. Phys. **43** (2010) 215101.

[8] V. Nam Do and P. Dollfus, J. Appl. Phys. **107** (2010) 063705.

[9] V. Hung Nguyen, A. Bournel, and P. Dollfus, J. Appl. Phys. **109** (2011) 093706.

[10] V. Hung Nguyen et al. Appl. Phys. Lett. **99** (2011) 042105.

[11] J. Bai, X. Zhong, S. Jiang, Y. Huang, and X. Duan, Nat. Nanotechnol. **5** (2010) 190.

[12] V. Hung Nguyen et al., Nanotechnol. **23** (2012) 065201

Figures

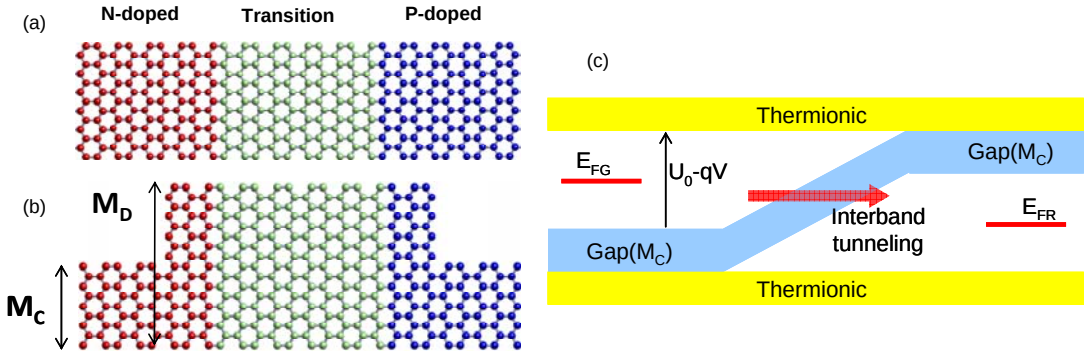

Figure 1. Schematic view of (a) armchair pn junction and (b) T-like pn junction with reduced bandgap in the transition region. (c) Schematic band profile of a graphene pn junction with uniform bandgap.

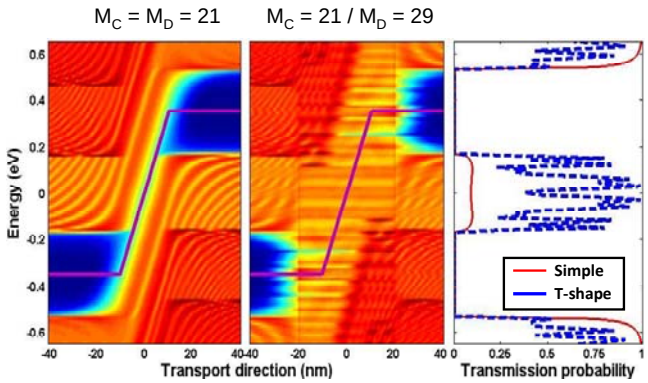

Figure 2. Local DOS of simple ($M_C = M_D$) and T-junctions ($M_D > M_C$ and (right) corresponding transmission probability.

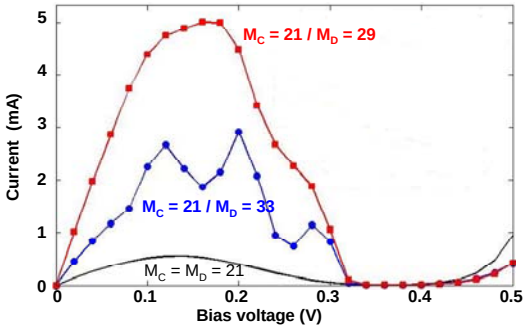

Figure 3. I-V characteristics (a) of the T-junctions with different indexes M_D. (L = 10.2 nm).

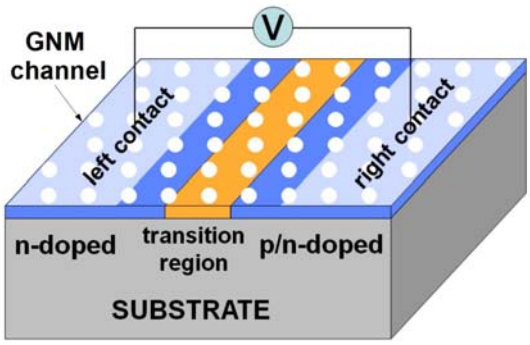

Figure 4. Schematic view of GNM Esaki diode.

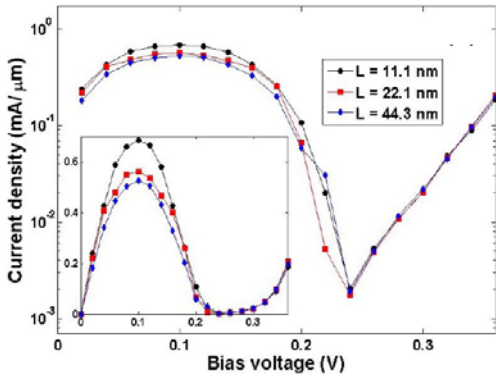

Figure 5. I-V characteristics of GNM devices with different transition lengths.

Acknowledgments: This work was supported by the ANR (projects NANOSIM_GRAPHENE and MIGRAQUEL).